Electronic Supporting Information

A Highly Active and Cr-Resistant Infiltrated Cathode for Practical Solid Oxide Fuel Cells

Tianrang Yang, Yeting Wen, Tao Wu, Nansheng Xu and Kevin Huang*

Experimental Section

Preparation of SCT precursor solution

To make the infiltrated sample, we first used an aqueous solution containing Sr, Co and Ta precursors and infiltrated it into a prefabricated porous LSCF-GDC skeleton. To make the SCT precursor solution, citric acid (Sigma-Aldrich) was first dissolved in a de-ionized water, followed by adding a stoichiometric amount of $Sr(NO_3)_2$ (Alfa Aesar) and $Co(NO_3)_2{\cdot}6H_2O$ (Alfa Aesar) under stirring. A separate solution containing ethylene diamine tetraacetic acid (EDTA, Sigma-Aldrich) dissolved in a diluted ammonia water was then mixed with the above solution with a targeted pH of 8. A stoichiometric amount of $Ta(OC_2H_5)_5$ (Sigma-Aldrich) dissolved into a pure ethanol was then slowly added into the above solution to complete the solution preparation. In the final solution, the total metal-ions concentration was 0.2 M with a molar ratio of citric acid to EDTA to metal ions at 2:1:1 and a volumetric ratio of de-ionized water to ethanol ratio at 5:1.

Fabrication of symmetrical cells and single cells with SCT@LSCF-GDC cathode

The symmetrical cell was first fabricated by screen printing an LSCF-GDC ink (purchased from Fuelcellmaterials) on both sides of a 500-μm thick $Gd_{0.2}Ce_{0.8}O_{2-\delta}$ (GDC, Fuelcellmaterials) dense

pellet, followed by firing at 1100 ^{o}C for 2 h. Thus-fabricated electrode is porous and has an effective electrode geometric area of 1.27 cm^2 and a thickness of *ca.* 40 μm. To make the infiltrated cathode, a 10 μL of SCT solution per infiltration cycle was then applied dropwise into the porous LSCF-GDC skeleton, followed by thermal treatment at 80 ^{o}C and 500 ^{o}C for 1 h, respectively. The rate of SCT loading was ~ 2% per infiltration cycle. The infiltrated samples were finally fired at 1000 ^{o}C for 2 h to form a pure SCT phase and thin layer that covers completely the surface of LSCF-GDC skeleton at 20 wt% loading level (relative to LSCF-GDC). For all electrochemical testing, gold paste (c8829a, Heraeus) with silver mesh were attached as current collectors to both sides of the cells and cured at 600 ^{o}C for 1 h before testing.

The single cell was fabricated by first screen printing a homemade NiO-GDC (NiO:GDC=3:2 weight ratio) ink on one side of a 200-μm thick GDC dense pellet and firing at 1300 ^{o}C for 2 h. The commercial LSCF-GDC ink was then screen-printed on the other side of the GDC membrane and then fired at 1100 ^{o}C for 2 h. The same SCT infiltration procedure was applied to make the infiltrated cathode for the single cell testing.

Electrochemical Impedance Spectroscopy (EIS) to evaluate cathode *performance*

The EIS spectra of symmetrical cells under OCV condition were collected as a function of temperature, atmosphere and time with a Solartron 1470/1455B multi-channel electrochemical station in a frequency range of 0.1 Hz - 1 MHz and AC amplitude of 10 mV. The collected EIS spectra were analyzed with equivalent circuit method by ZSimpWin software to extract the polarization resistance of interest.

The study of the effects of air contaminants such as Cr, H_2O and CO_2 on the oxygen electrocatalysis performance of the SCT@LSCF-GDC is practically important. To ensure a fair

comparison, each study was carried out on two side-by-side sister cells in the same furnace, one for the untreated cathode and one for the infiltrated cathode. The Cr-effect on cathodic polarization resistance R_P was carried out isothermally as a function of time. After the initial Cr-free operation at 700 ^oC for 234 hours, the cells were cooled down to room temperature and a large piece ferritic steel 430 sheet (W2″×T0.1″×L24″, a common metal interconnect for SOFCs) as a Cr-source was coiled and inserted into the upstream of a flowing air. The H_2O and CO_2 effects on R_P were carried out in the same side-by-side sister cell configuration, but over a temperature range from 550 to 700 ^oC. The concentrations were varied from 0 to 5.5% for H_2O and 0 to 1.1% for CO_2, respectively. It usually takes 2-hour to stabilize after each gas switching. To avoid additional contaminants from the ambient air, a commercial synthetic air was used for this study.

Microstructure and phases characterization

The microstructures of electrodes were characterized by a field emission scanning electron microscope (FESEM, Zeiss Ultraplus). To observe the cross-section of the infiltrated cathode, Focused Ion Beam (FIB, Hitachi NB-5000) technique was used to prepare samples and transmission electron microscope (TEM) imaging (Hitachi H-9500), selected area electron diffraction (SAED) and scanning transmission electron microscope (STEM, Hitachi HD-2000) imaging equipped with energy-disperse x-ray spectroscopy (EDX) were employed to obtain images, determine crystal structure as well as analyze chemical compositions. The resolutions of STEM-EDX are 0.8, 0.5 and 0.3 nm for spot, line-scan and mapping modes, respectively. To analyze the surface chemistry, particularly Sr-concentration of cathode, X-ray photoelectron spectroscopy (XPS) (Kratos AXIS Ultra DLD XPS) was performed. To ensure the accuracy, the binding energy (BE) was calibrated by the C-1s photoemission peak at 284.6 eV.

The phase composition of the prepared powder sample was examined with an X-ray diffractometer (Rigaku MiniFlex Ⅱ) equipped with Cu Kα radiation (λ=1.5418 Å) over a 2θ=10 - 90° range with a step size of 0.02° and a scanning rate of 5° min^{-1}. The Raman spectra were collected by a LabRam/HR confocal Raman system (LabRam Invers, Horiba Jobin-Yvon) equipped with a 632.8 nm He–Ne laser.

Computational Methods

DFT-based Calculations for Gibbs Free Energy Change of Chemical Reactions

All the ground-state electronic calculations were performed by Perdew-Burke-Ernzerhof (PBE) generalized gradient approximation (GGA) exchange-correlation implemented in the Vienna *ab* Initio Simulation Package (VASP).[1-3] The projector-augmented-wave (PAW) method was adopted with valence configurations of O ($2s^2 2p^4$), Cr ($3d^5 4s^1$), Co ($3d^8 4s^1$), Sr ($4s^2 4p^6 5s^2$) and Ta ($5d^3 6s^2$).[4,5] Electronic structure was described in a plane-wave basis with a kinetic energy cut-off of 500 eV. For pure metal calculation, such as Co, the standard DFT calculation was employed. For the transition metal oxides calculation such as $SrCo_{0.9}Ta_{0.1}O_3$, Cr_2O_3, $SrCrO_4$, Co_3O_4, we employed the GGA+*U* formalism to account for strong on-site coulombic interactions of the 3d-electrons.[6] The value of *U* for Co and Cr were set to 3.3 and 3.5 based on previous work. The lattice constants and atomic positions were both fully relaxed until reaching a maximum energy difference and residual force on atoms converge at 10^{-4} eV and 10^{-3} eV/Å, respectively. We used a *k*-point grid of > (1000)/*n* points, where *n* represents the number of atoms in the unit cell, for a uniform atomic distribution in *k*-space with a gamma-centered grid.

The Gibbs free energy (G) can be calculated by:

$$G = F + PV \quad \text{(S1)}$$

where F is the Helmholtz free energy, PV term is the product of pressure (P) and volume (V). PV term is neglected due to its small change for solid-state materials; the Gibbs free energy change is approximated to the change of Helmholtz free energy. The Helmholtz free energy is calculated by:

$$F = E_0 + E_{vib}(T) - TS_{vib} \quad \text{(S2)}$$

where E_0 is the DFT total energy at 0K, $E_{vib}(T)$ is phonon vibration energy, T is the temperature and S_{vib} is the phonon vibration entropy. To obtain the phonon vibration energy and phonon vibration entropy, phonon frequency calculations were carried out by implementing force constants in the PHONOPY code.[7] The force constants were obtained by density functional perturbation theory (DFPT) method as implemented in VASP.[8]

It should be noted that the total energy calculations were for periodic solids at 0 K. Since O_2 is gaseous under the standard state, the energies of O_2 was adjusted using Wang's method.[9] In addition, energies from calculations with the +*U* correction were not comparable to those without +*U*. Hence, we use GGA when appropriate, GGA+*U* otherwise, and mix energies from the two calculation methodologies by adding energy correction term to the GGA+*U* calculations for better comparisons.

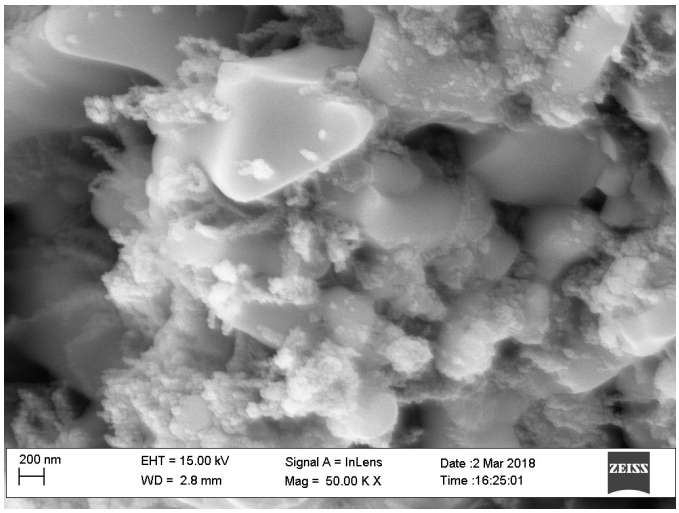

Figure S1. SEM image of SCT@LSCF after calcination at 800 ^{o}C for 2 h.

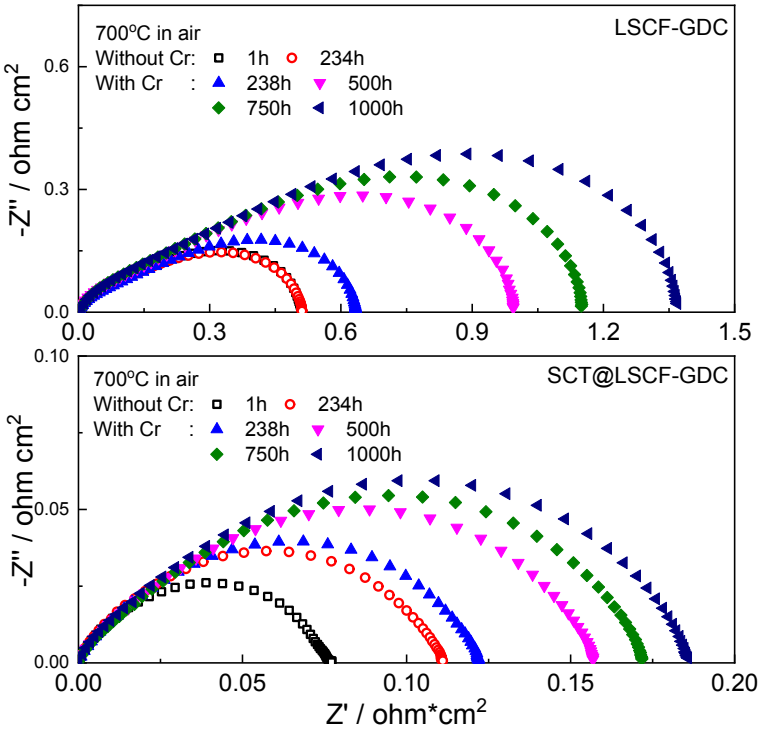

Figure S2. Time-dependent EIS spectra of the untreated and infiltrated cathodes.

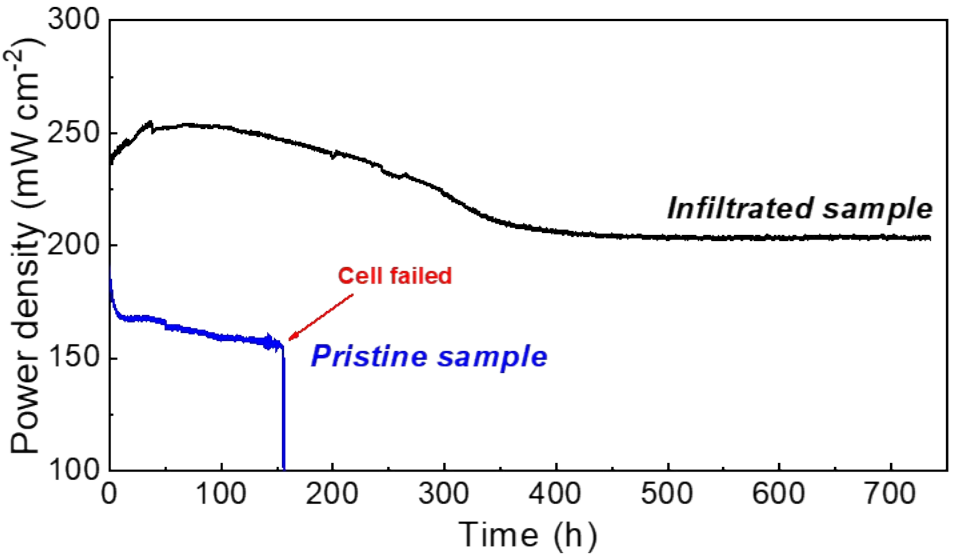

Figure S3. Single cell performance of cells with LSCF-GDC (untreated) or SCT10@LSCF-GDC as cathodes, GDC as electrolyte and Ni-GDC as fuel electrode at 700 ^{o}C. Test conditions: 100 SCCM 97%H_2/3%H_2O, static air, potentiostatic running at 0.65 V.

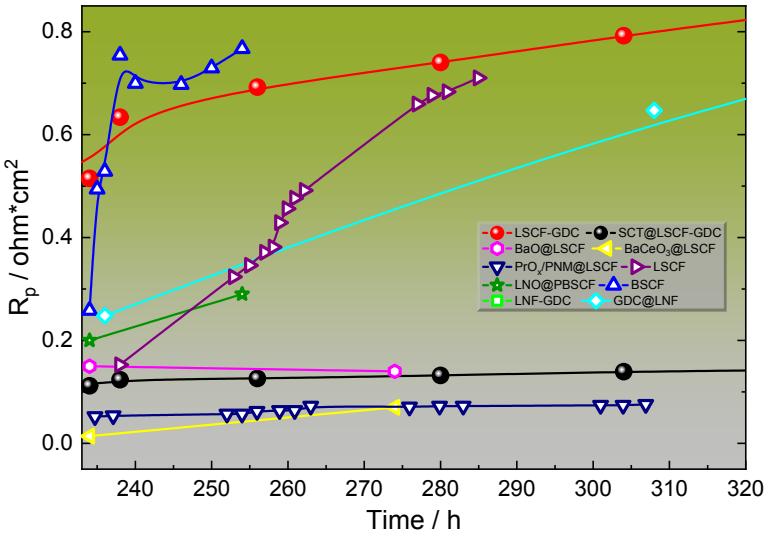

Figure S4. R_p in Cr-containing atmosphere for the state-of-the-art cathodes; the starting time are normalized to this work.

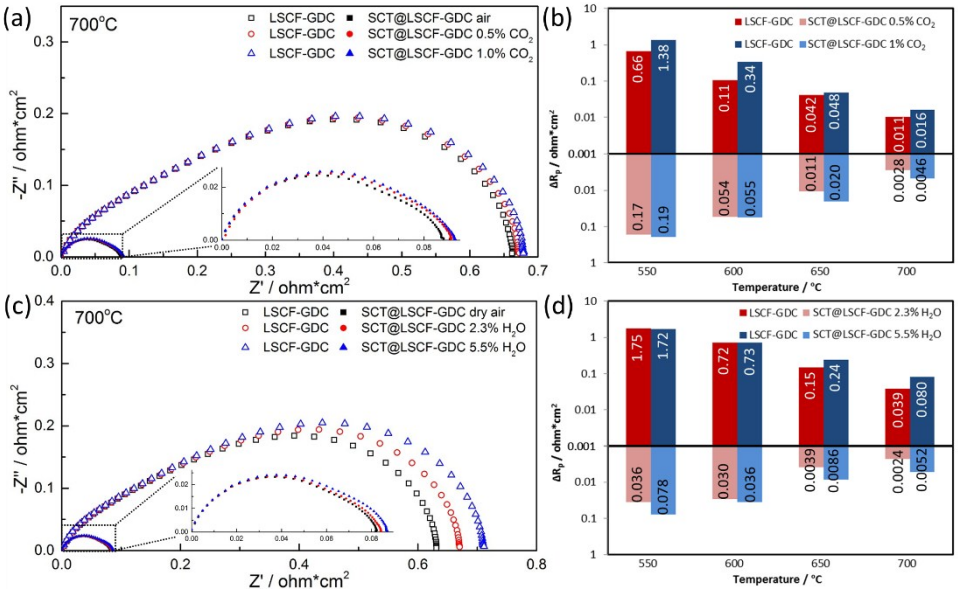

Figure S5. (a)&(c) Impedance spectra of untreated and infiltrated symmetrical cells measured at 700 °C under CO_2 and H_2O containing air, respectively; (b)&(d) temperature-dependent change of R_P by the exposure to CO_2 and H_2O containing air, respectively.

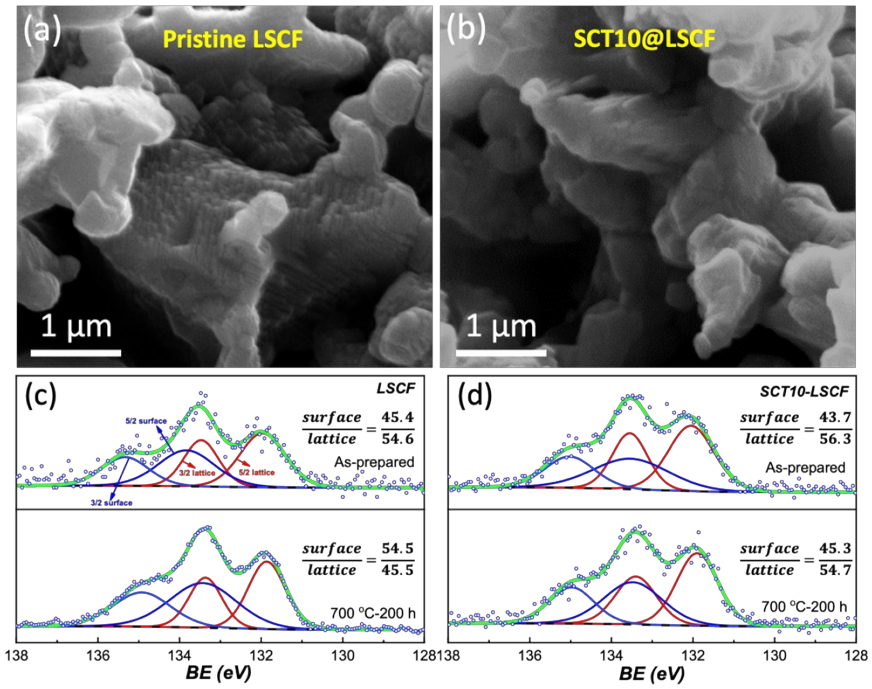

Figure S6. The SEM morphology after 5,000 h annealing at 700 °C of (a) LSCF and (b) SCT@LSCF. The Sr-3*d* XPS spectra of untreated LSCF (c) and SCT@LSCF (d) before and after annealing in air at 700 °C for 200 h.

Figure S6 (a) and (b) show a sign of segregated Sr-species in the untreated LSCF-GDC as rough surface, but not in SCT@LSCF-GDC after 5,000 h annealing. To further support this preliminary SEM observation, XPS was performed to examine the surface Sr-concentration on a sister-set of the samples annealed at 700 °C for only 200 h. The rationale is that there will be more pronounced Sr-segregation for the sample tested for 1,000 h if the sample treated at 700 °C for 200 h is found with surface Sr-segregation. Figure S6 (c) shows Sr-3d XPS spectrum of the untreated LSCF-GDC sample, indicating that the ratio of (surface-Sr)/(lattice-Sr) increases from 45.4/54.6 to 54.5/45.5 after the treatment. In contrast, Figure S6 (d) of Sr-3d XPS spectrum of SCT10@LSCF-GDC shows an almost constant ratio after the same treatment.

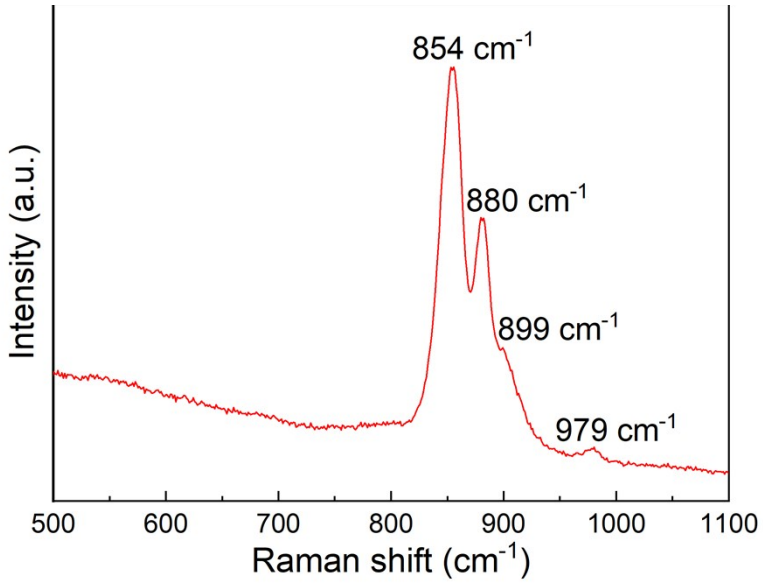

Figure S7. Raman spectra LSCF pellet after annealing at 900 °C for 100 h in Cr-rich air. The Raman shifts at 854 cm^{-1}, 880 cm^{-1} and 899 cm^{-1} correspond to $SrCrO_4$.[10-11]

References

1. G. Kresse and J. Furthmüller, *Phys. Rev. B*, 1996, **54**, 11169-11186.
2. G. Kresse and J. Hafner, *Phys. Rev. B*, 1994, **49**, 14251-14269.
3. G. Kresse and J. Hafner, *Phys. Rev. B*, 1993, **47**, 558-561.
4. G. Kresse and D. Joubert, *Phys. Rev. B*, 1999, **59**, 1758-1775.
5. P. E. Blöchl, *Phys. Rev. B*, 1994, **50**, 17953-17979.
6. V. I. Anisimov, F. Aryasetiawan and A. Lichtenstein, *J. Phys. Condens. Matter*, 1997, **9**, 767-808.
7. A. Togo and I. Tanaka, *Scr. Mater.,* 2015, **108**, 1-5.
8. P. Giannozzi, S. de Gironcoli, P. Pavone and S. Baroni, *Phys. Rev. B*, 1991, **43**, 7231-7242.
9. L. Wang, T. Maxisch and G. Ceder, *Phys. Rev. B,* 2006, **73**, 195107.
10. A.E. Hughes, S.Mayo, Y.S.Yang, T. Markley, S.V. Smith, S. Sellaiyan, A. Uedono, S.G. Hardin and T.H. Muster, *Progress in Organic Coatings,* 2012, **74**, 726-733.

11. F.H. Scholes, S.A. Furman, A.E. Hughes, T. Nikpour, N. Wright, P.R. Curtis, C.M. Macrae, S. Intem and A.J. Hill, *Progress in Organic Coatings,* 2006, **56**, 23-32.